Two Equivalent Internal Rotations in the Microwave Spectrum of 2,6-Dimethylfluorobenzene

Safa Khemissi, Ha Vinh Lam Nguyen

Two Equivalent Internal Rotations in the Microwave Spectrum of 2,6-Dimethylfluorobenzene

Safa Khemissi and Ha Vinh Lam Nguyen*

Abstract: Large amplitude motion of methyl groups in isolated molecules is a fundamental phenomenon in molecular physics. The methyl torsional barrier is sensitive to the steric and electronic environment in the surrounding of the methyl group, making the methyl group a detector of the molecular structure. To probe this effect, the microwave spectrum of 2,6-dimethylfluorobenzene, one of the six isomers of dimethylfluorobenzene, was measured using two pulsed molecular jet Fourier transform microwave spectrometers operating in the frequency range from 2 to 40 GHz. Due to internal rotations of two equivalent methyl groups with relatively low torsional barriers, all rotational transitions split into quartets with separations of up to several hundreds of MHz. The splittings were analyzed and modeled to deduce a torsional barrier of 236.7922(21) cm^{-1}. The results are compared to those obtained from quantum chemical calculations and with other fluorine substituted toluene derivatives of the current literature where the methyl group is adjacent to the fluorine atom.

1. Introduction

The importance of toluene and its derivatives in spectroscopic, theoretical, and application researches has been proven by an enormous number of studies in those fields. Especially for spectroscopy, the rotational spectrum of toluene has always attracted attention since its microwave spectrum was recorded and analyzed for the first time by Rudolph *et al.*[1] Not only the structure of toluene was determined to great accuracy, several theoretical models and program codes have been also developed to reproduce the V_6 potential arising from the internal rotation of the C_{3v} methyl group attached to a phenyl frame with C_{2v} symmetry.[2-5] To gain insights into the substitution effect on this large amplitude motion (LAM) of toluene, studies on many fluorinated derivatives have been performed, such as the investigations on three isomers of fluorotoluene,[6-8] a systematic microwave investigation on the six isomers of difluorotoluene,[9-13] and the work on two isomers of trifluorotoluene.[14] All these studies have shown a variety of the potentials of the methyl torsion in both shape and height, which depend on the substituted position(s) of the fluorine atom(s). For example, due to symmetry, *p*-fluorotoluene has a V_6 potential with a very low hindering barrier of 4.8298(54) cm^{-1}.[8] The *ortho* isomer with its V_3 potential of 227.28(2) cm^{-1} could be easily modeled.[6] Finally, *m*-fluorotoluene has remained over half a century a challenge due to the values of V_3 and V_6 terms which are comparable in magnitude.[7]

S. Khemissi M. Sc., Dr. H. V. L. Nguyen*
Laboratoire Interuniversitaire des Systèmes Atmosphériques (LISA), CNRS UMR 7583, Université Paris-Est Créteil, Université de Paris, Institut Pierre Simon Laplace, 61 avenue du Général de Gaulle, F-94010 Créteil, France
*E-mail: lam.nguyen@lisa.u-pec.fr

Supporting information for this article is given via a link at the end of the document.

Investigations on toluene derivatives with two methyl groups attached on the phenyl ring are scarce, such as those on the three isomers of dimethylbenzaldehyde[15] and the three isomers of dimethylanisole.[16-18] The reason is probably the complexity of the microwave spectrum due to the coupled LAMs of the two methyl groups, which makes it hard to assign and to model. As a consequence, effective Hamiltonians often have to be included to reproduce the experimental spectra with sufficient accuracy.

The systematic investigations on dimethylanisoles have indicated some problems associating with the oscillation motions of the methoxy group which is suspect to influence the internal rotation of the two methyl groups.[16-18] The same effects could also happen in dimethylbenzaldehyde or other derivatives, whenever a group of more than two atoms are attached on the phenyl ring in addition to the two methyl groups. Therefore, we decided to study the dimethylfluorobenzene family, where the third substitution is a fluorine atom and the molecular planarity becomes evident. Here, we report the results for the first member of the family, 2,6-dimethylfluorobenzene (26DMFB). An interesting character of 26DMFB is its C_{2v} symmetry with the presence of two equivalent internal rotors with a relatively low torsional barrier. Consequently, all rotational levels split into quartets with separation of up to hundreds of MHz between the torsional components, making the assignment of the microwave spectrum challenging. The present study on 26DMFB adds a contribution to the very limited number of investigations on C_{2v} molecules showing methyl internal rotations reported in the literature, which are acetone,[19] dimethyl ether,[20] diethyl ketone,[21] 2,5-dimethylfuran,[22] 2,5-dimethylthiophene,[23] and dimethyl sulfide.[24]

2. Theoretical Section

2.1. Quantum Chemical Calculations

Three quantum chemistry levels of theory were used to calculate the rotational constants using the *Gaussian 16* program package[25] to support the experimental work. The first level uses the second order Møller-Plesset perturbation method (MP2) and the split-valence triple-zeta basis set 6-31G(d,p). Many studies on aromatic or aromatic ring containing molecules such as phenetole,[26] *o*-methylanisole,[27] 2-ethylfuran,[28] coumarin,[29] quinolone,[30] and isoquinoline[30] have shown that the rotational constants predicted using this combination were accidentally very close to the experimental values. For comparison, we also applied the Kohn-Sham density functional theory[31] using Becke's three parameter hybrid exchange functional[32] and the Lee-Yang-Parr correlation functional[33] (B3LYP), as our experiences and several studies in the literature have shown that this method is adequate for predictive guidance of phenyl ring containing molecules.[14,17-34] Grimme's distortion

corrections[35] and Becke-Johnson damping[36] were used in addition, and the basis set 6-311++G(d,p) was chosen. We also carried out optimizations at the MP2/6-311++G(d,p) level of theory, a method quite often used in the spectroscopic community.[37-39] The optimized geometry of 26DMFB is given in Figure 1. The atomic Cartesian coordinates are collected in Table S-1 of the Supplementary Material. The obtained equilibrium rotational constants are summarized in Table 1. Vibrational frequency calculations in the harmonic approximation confirmed that the optimized geometry is indeed a minimum and not a saddle point. Anharmonic frequency calculations were carried out to obtain vibrational ground state rotational constants and quartic centrifugal distortion constants.

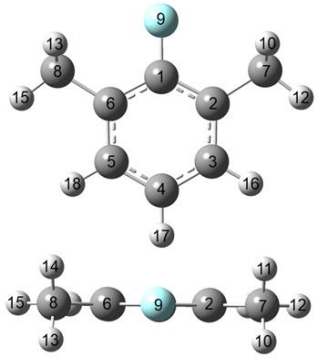

Figure 1. The molecular geometry of 26DMFB optimized at the MP2/6-31G(d,p). Upper figure: front view. Lower figure: view along the F(9)–C(1) bond.

Successful assignment of the experimental spectrum for each molecule requires precisely predicted rotational constants using quantum chemistry. For 26DMFB the assignment was made using rotational constants calculated at MP2/6-31G(d,p) level, as will be described later in section 3.2. To find alternatives other than MP2/6-31G(d,p), geometry optimizations with the MP2 and B3LYP methods in combination with different basis sets were carried out. In addition, we also tried other methods such as Truhlar's M06-2X[40] and coupled cluster (CCSD).[41] The results obtained at all levels of theory in use are grouped in Table S-2 of the Supplementary Material.

Table 1. Equilibrium rotational constants A_e, B_e, C_e (in MHz), vibrational ground state rotational constants A_0, B_0, C_0 (in MHz) and centrifugal distortion constants (in kHz) in the symmetrically reduced Hamiltonian obtained from anharmonic frequency calculations, equilibrium dipole moment component μ_b (in Debye), and the V_3 potential term (in cm^{-1}) calculated at the MP2/6-31G(d,p), MP2/6-311++G(d,p), and B3LYP-D3BJ/6-311++G(d,p) levels of theory.

	MP2/6-31G(d,p)	MP2/6-311++G(d,p)	B3LYP-D3BJ/6-311++G(d,p)
A_e	2234.1	2234.3	2245.4
B_e	1780.6	1766.4	1772.4
C_e	1003.1	998.7	1002.8
A_0	2223.0	2220.0	2231.9
B_0	1766.8	1751.7	1759.1
C_0	996.7	991.1	995.9
D_J	0.12164	0.12348	0.12368
D_{JK}	–0.18236	–0.18466	–0.18763
D_K	0.07269	0.07339	0.07618
d_1	–0.00206	–0.00268	–0.00327
d_2	–0.00102	–0.00131	–0.00122
μ_b	1.26	0.98	1.03
V_3	207.0	245.2	213.0

The energy potential function of the methyl internal rotations was performed for only one methyl group because of the C_{2v} molecular symmetry by varying the dihedral angle $\alpha_1 = \angle(C_1,C_2,C_7,H_{12})$ in a grid of 10° while all other geometry parameters were allowed to vary. A rotation span of 120° was sufficient due to the C_{3v} symmetry of the methyl group. The obtained potential energy points were parameterized with a one-dimensional (1D) Fourier expansion and then drawn as a contour plot given in Figure S-1 in the Supplementary Material.

Finally, to study the coupling of the two methyl internal rotations, a 2D potential energy surface (PES) depending on α_1 and $\alpha_2 = \angle(C_1,C_6,C_8,H_{15})$ was performed. The dihedral angles α_1 and α_2 were varied over a grid of 10°; all other geometry parameters were optimized at the B3LYP-D3BJ/6-311++G(d,p) level of theory. The corresponding energies were parameterized with least squares fits of a 2D-Fourier series as

$$V(\alpha) = -410.266011\ Hartree + \frac{233\ cm^{-1}}{2}[cos(3\alpha_1) + cos(3\alpha_2)] + 10.6\ cm^{-1} \cdot cos(3\alpha_1)cos(3\alpha_2). \quad (1)$$

The PES could be drawn as a contour plot visualized in Figure 2. The Fourier coefficients indicated that the coupling term between the two LAMs is less than 5% of the V_3 potential terms. A similar situation was found for the PES calculated at the MP2/6-31G(d,p) and the MP2/6-311++G(d,p) levels illustrated in Figure S-2 of the Supplementary Material.

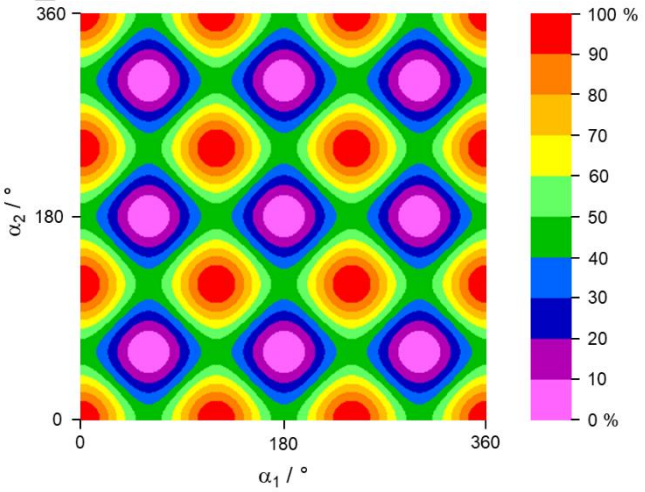

Figure 2. The potential energy surface of 26DMFB in dependence on the two dihedral angles α_1 and α_2, describing the torsions of the two equivalent methyl groups. The angles α_1 and α_2 were varied in steps of 10° while all other geometry parameters were optimized at the B3LYP-D3BJ/6-311++G(d,p) level of theory. The numbers in the color code indicate the energy in percent relative to the lowest energy conformation at E_{min} = –410.267021 Hartree (0%). The energy maximum is at E_{max} = –410.264905 Hartree (100%).

2.2. Symmetry considerations

If a molecule with C_{2v} point-group symmetry at equilibrium undergoes internal rotations of two equivalent methyl groups, as in the case of 26DMFB, its appropriate molecular symmetry group is G_{36} with the known labeling scheme A_i, E_i, and G (i = 1 – 4).[42] An alternative labeling scheme of G_{36} has been proposed for 2,5-dimethylthiophene using the semi-direct product $(C_3^I \otimes C_3^I) \circledS C_{2v}$.[23] The superscript I denotes the intrinsic group of the internal rotors, and the first part thus indicates the direct product $C_3^I \otimes C_3^I$ of the two intrinsic C_3 groups. This part

decomposes into four orbits (σ_1,σ_2) under C_{2v}. One representative of each orbit forms the first part of the symmetry label, e.g. (00), which can be used instead of the full symmetry label given in Table 1 of Ref. [23] if the quantum numbers K_a and K_c are known. We will use the same notation for 26DMFB. The abbreviated symmetry labels (00), (01), (11), and (12) correspond to the A_i (i = 1 – 4), G, E_3 and E_4, and E_2 and E_3, respectively, [42] given under the column S2 in Table 1 of Ref. [23].

The 9 protons in 26DMFB result in 512 nuclear spin functions. The representation Γ_{ns} is the product of Γ_1 = 10 (00)·A_1 + 6 (00)·B_2 + 3 (12)·A′ + (12)·A″ + 3 (11)·A + (11)·B + 8 (01)·A for the (10 11 12) and (13 14 15) triples, Γ_2 = 3 (00)·A_1 + (00)·B_2 for the (16 18) pair, and Γ_3 = (00)· A_1 for the (17) proton, resulting in Γ_{ns} = 36 (00)·A_1 + 28 (00)·B_2 + 10 (12)·A′ + 6 (12)·A″ + 10 (11)·A + 6 (11)·B + 32 (01)·A. We determined the spin weights by the number of allowed total wave functions for $\Gamma_{el} = \Gamma_{vib}$ = (00)·A_1, which is the same as given in Table 3 of Ref. [23] with four torsional components of two different *b*-type transitions. If only the spin statistical weight is considered, the (01) torsional component is the strongest with the spin weight of 64, followed by the (00) species with 36. The spin weight of the (11) component is only 20 for K_aK_c = ee ↔ oo (e = even, o = odd) transitions and 12 for eo ↔ oe transitions, similar to the weight of 20 for the (12) species.

3. Microwave spectroscopy

3.1. Measurements

At the beginning of the experiment, a broadband scan in the frequency range from 10.0 to 13.4 GHz was carried out. A portion of the survey spectrum from 12150 MHz to 12450 MHz is shown in Figure 3, which captures all torsional components of the $3_{31} \leftarrow 2_{20}$ rotational transition quartet. All signals appearing in the broadband scan were later remeasured at higher resolution. The estimated uncertainty is better than 2 kHz for intense, unblended lines while transitions separated less than 5 kHz are not resolved. Due to spin-spin or spin rotation coupling of 9 hydrogen atoms in 26DMFB, many lines appear quite broad and many show additional splittings up to 20 kHz. The measurement accuracy is estimated to be about 4 kHz.

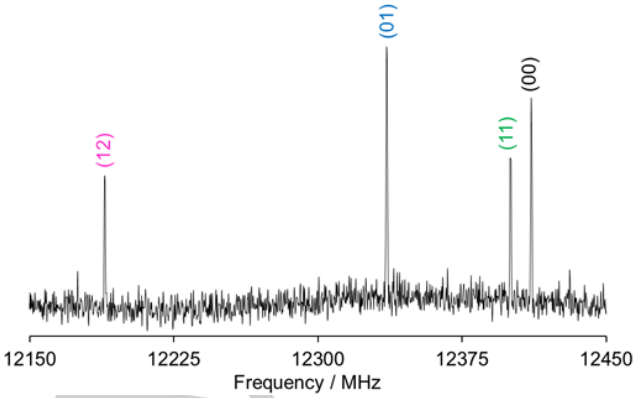

Figure 3. A part of the survey spectrum of 26DMFB from 12150 to 12450 MHz capturing all four torsional components (00), (01), (12), and (11) of the rotational transition $3_{31} \leftarrow 2_{20}$. The arbitrary intensity is given in a logarithmic scale. The (01) torsional component is the strongest, followed by the (00) component, while the (11) and (12) species are weakest, in agreement with the spin statistical weight.

3.2. Spectrum Assignment and Fits

Results from quantum chemical calculations have shown that 26DMFB has only one dipole moment components in the *b*-direction due to its C_{2v} molecular symmetry. Only *b*-type transitions are expected in the microwave spectrum. In the first step, using the rotational constants calculated at the MP2/6-31G(d,p) level, the rigid rotor spectrum was predicted in the frequency range of 10.0 to 13.4 GHz using the *XIAM* code[43] and compared to the survey spectrum. Some transitions with low K_a such as $5_{05} \leftarrow 4_{14}$, $5_{15} \leftarrow 4_{04}$, $6_{06} \leftarrow 5_{15}$, and $6_{16} \leftarrow 5_{05}$ could be assigned readily because their positions were predicted quite accurately. Symmetry considerations have shown that four torsion components (00), (01), (11), and (12) are expected due to the internal rotations of two equivalent methyl groups in 26DMFB. In the second step, a prediction taking into account these LAM effects was performed. The initial V_3 potential as well as the angles $\angle(i,a)$ between the internal rotor axes and the principal *a*-axis were taken from the calculated values. Since checking the assignment with combination difference loops was not possible because only *b*-type transitions are allowed, we verified the assigned frequencies by Separately Fitting the Large Amplitude Motion Species using the program *SFLAMS*.[44] The lines of the (00) symmetry species follow a rigid rotor pattern and could be fitted well to a standard deviation of 2.3 kHz using an effective Hamiltonian $H = H_r + H_{cd}$ comprising rotational and quartic centrifugal distortion terms of Watson's S reduction in its I^r representation.

The assignments of the (01), (11), and (12) species lines were also checked with *SFLAMS* using the additional odd power term

$$H_{op} = \left(q + q_J P^2 + q_K P_a^2\right) P_a + r P_b \qquad (2)$$

in the Hamiltonian, where *P* is the angular momentum operator with its components P_a, P_b, P_c referring to the principal axes of inertia *a*, *b*, and *c*. The parameters *q* and *r* are sometimes called D_a and D_b in the literature and the higher order terms q_J and q_K can be also found as D_{aJ} and D_{aK}. The separate *SFLAMS* fits for the (01), (11), and (12) species achieved a standard deviation of 1.8 kHz, 2.1 kHz, and 3.4 kHz, respectively. The four separate fits are given in Table 2.

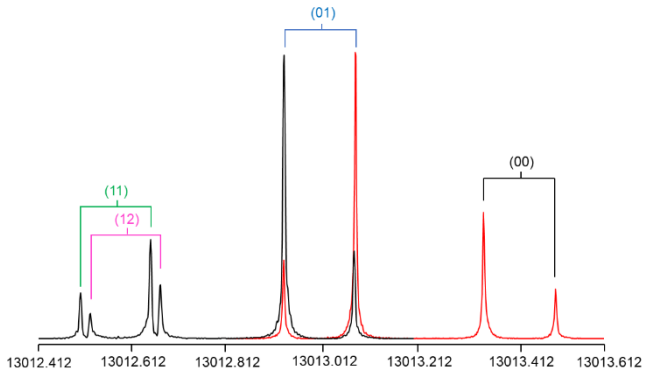

Figure 4. Typical spectra of the $6_{06} \leftarrow 5_{15}$ transition of 26DMFB recorded at high resolution. The frequencies are in MHz. The torsional components are given in parentheses; the Doppler pairs are marked by brackets. Two spectra are overlapped as can be distinguished by different colors and the intensity is normalized. For each spectrum, 50 decays were co-added.

Table 2. Molecular parameters of the (00), (01), (11), and (12) species obtained with the *SFLAMS* program.

Par.[a]	Unit	Fit (00)	Fit (10)	Fit (11)	Fit (12)
A	MHz	2248.67572(11)	2247.74284(17)	2246.80605(18)	2246.80684(12)
B	MHz	1771.52199(11)	1771.34039(13)	1771.6033(17)	1771.160233(98)
C	MHz	1002.904778(56)	1002.908841(46)	1002.912893(83)	1002.912873(51)
D_J	kHz	0.05349(77)	0.05506(88)	0.0288(67)	0.05802(79)
D_{JK}	kHz	0.1029(28)		0.166(36)	0.0185(46)
D_K	kHz	0.0467(30)	0.1952(88)	–0.080(30)	0.0259(81)
d_1	kHz	–0.02892(42)	–0.02553(57)	–0.0247(13)	–0.02801(41)
d_2	kHz	–0.00861(17)	–0.00448(17)	–0.0163(24)	–0.00542(21)
q	MHz		42.30769(79)	–39.0884(49)	84.69308(40)
q_J	kHz		–1.626(61)		–3.546(26)
q_K	kHz		–3.565(80)		–5.936(36)
r	MHz		19.5312(73)		
N[b]		114	87	112	104
σ[c]	kHz	2.3	1.8	3.4	2.1

[a] All parameters refer to the principal axis system. Watson's S reduction and I^r representation were used. The values of all parameters which were not fitted were set to zero.
[b] Number of lines.
[c] Standard deviation of the fit.

In total, 417 torsional species lines were identified and input in the program *XIAM*. The three rotational constants, five centrifugal distortion constants, the V_3 term, the angles $\angle(i,a)$, and the three higher order terms $D_{2\pi J}$, $D_{2\pi K}$, and $D_{2\pi -}$, which describe the empirical internal rotation-overall rotation distortion in the principal axis system, were fitted, yielding a standard deviation of 4.0 kHz. The molecular parameters are collected in Table 3. The complete list of all fitted rotational transitions along with their residuals is given in Table S-3 of the Supplementary Material.

Table 3. Molecular parameters of 26DMFB as obtained with the program *XIAM*.

Par.[a]	Unit	Fit *XIAM*	Calc.[b]
A	MHz	2247.42817(13)	2245.4
B	MHz	1771.27166(12)	1772.4
C	MHz	1002.889238(58)	1002.8
D_J	kHz	0.05441(72)	0.12368
D_{JK}	kHz	0.0513(30)	–0.18763
D_K	kHz	0.0341(39)	0.07618
d_1	kHz	–0.02744(39)	–0.00327
d_2	kHz	–0.00647(16)	–0.00122
V_3	cm^{-1}	236.7922(21)	213.0
$D_{2\pi J}$	MHz	0.06926(21)	
$D_{2\pi K}$	MHz	–0.06299(45)	
$D_{2\pi -}$	MHz	0.04710(19)	
$\angle(i,a)$[c]	deg	30.4282(30)	31.5727
$\angle(i,b)$	deg	59.5718(30)	58.4273
$\angle(i,c)$	deg	90.00[d]	90.0000
N[e]		417	
σ[f]	kHz	4.0	

[a] All parameters refer to the principal axis system. Watson's S reduction and I^r representation were used.
[b] Calculated at the B3LYP-D3BJ/6-311++G(d,p) level of theory. The rotational constants refer to the equilibrium structure. The vibrational ground state constants are given in Table 1. Centrifugal distortion constants are obtained from anharmonic frequency calculations.
[c] The angle $\angle(i_2,a)$ for the second rotor is derived from the relation $\pi - \angle(i_1,a)$.
[d] Fixed due to symmetry.
[e] Number of lines.
[f] Standard deviation of the fit.

4. Discussion

The global fit obtained with the program *XIAM* including 417 torsion transitions reaches a standard deviation of 4.0 kHz, which is the estimated measurement accuracy. All molecular parameters are accurately determined. Because of the strong correlation with the V_3 term, the internal rotational constants F_0 of the methyl tops were fixed at 158 GHz, a value often found for methyl groups. We note that F_0 could be fitted, but its correlation with the V_3 term is 1.000 because only transitions of the vibrational ground state are available in the data set.

Comparison of the experimental rotational constants with those predicted by different combinations of methods and basis sets given in Table S-2 of the Supplementary Material shows that results from the majority of levels agree well with the experimental ones. The error compensations at the B3LYP-D3BJ/6-311++G(d,p) level of theory yield B_e constants which are in almost exact agreement with the experimental values. Though it is not physically meaningful to compare predicted B_e constants with experimental B_0 constants, the B3LYP-D3BJ/6-311++G(d,p) level offers cost-efficient calculations with accidentally good accuracy to be useful in guiding the assignment of microwave spectra and is therefore recommended for other isomers of dimethylfluorobenzene. Theoretical B_0 rotational constants obtained by anharmonic frequency calculations (see Table 1) show larger deviations to the experimental values compared to the B_e constants. The reason is most probably the LAMs of 26DMFB which generally cannot be described correctly by calculations in electronic structure packages since in Cartesian coordinates, the triple-well potential in internal coordinates is assumed to be a quartic potential.

The barrier height of the two equivalent methyl tops is 236.7922(21) cm^{-1}. Comparison with values of other toluene derivatives given in Figure 5 where a fluorine atom and a methyl group are adjacent, we found that if the methyl torsion has the shape of a V_3 potential, the barrier height is always around 220 cm^{-1}, ranging from 190 cm^{-1} in 2,4,5-trifluorotoluene to 237 cm^{-1} in 26DMFB. Only in 2,6-difluorotoluene, the potential is V_6 due to symmetry.[13] As mentioned, the barrier hindering a methyl rotation is quite sensitive to many structural and electronic effects. In a systematic investigation on a series of methyl alkyl ketones, Andresen et al. proposed a link between the torsional barrier of the acetyl methyl group and the molecular structure at the other side of the carbonyl bond. A "pseudo-C_s" conformation leads to a barrier height of approximately 180 cm^{-1} and a C_1 conformation is connected to a value of about 240 cm^{-1}.[45-47] In another study, Herbers et al. pointed out that π-conjugations from the phenyl group significantly affect the acetyl methyl torsion of acetophenone derivatives and the barrier height raises to 600 cm^{-1}.[44] Obviously, the methyl torsional barrier can be applied as a direct measure for steric and electronic contributions in the molecules.

The torsional barriers of 26DMFB calculated at the MP2/6-31G(d,p), MP2/6-311++G(d,p), and B3LYP-D3BJ/6-311++G(d,p) levels given in Table 1 are in good agreement with

the experimental value, whereby the value obtained from the MP2/6-311++G(d,p) level matches best. It is frequently observed for toluene derivatives, e.g. the three isomers of methylanisole, that the B3LYP functional performs well in predicting molecular geometry while the MP2 method yields better results for the torsional barrier.[16,27,34] However, if the values from the 2D-PES parameterizations are considered (see equation (1) and Figure S-2), the value of 233 cm^{-1} calculated at the B3LYP-D3BJ/6-311++G(d,p) level is very accurate.

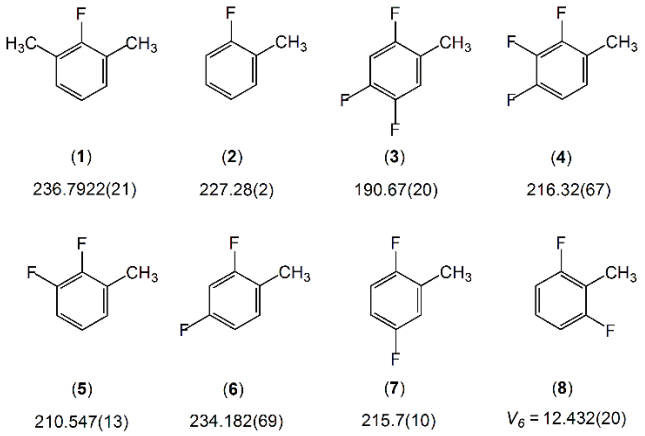

Figure 5. Comparison of the methyl torsional barrier of two equivalent methyl groups in 26DMFB with the values of other toluene derivatives where the fluorine atom and the methyl group are adjacent. (**1**) 26DMFB (this work), (**2**) 2-fluorotoluene,[6] (**3**) 2,4,5-trifluorotoluene,[14] (**4**) 2,3,4-trifluorotoluene,[14] (**5**) 2,3-difluorotoluene,[9] (**6**) 2,4-difluorotoluene,[10] (**7**) 2,5-difluorotoluene,[11] and (**8**) 2,6-difluorotoluene.[13]

5. Conclusion

The two equivalent methyl groups of 26DMFB undergo internal rotation with torsional splittings of all rotational transitions into quartets, which were observed and analyzed using a combination of microwave spectroscopy and quantum chemistry. The assignments were checked by separately fitting the four large amplitude motion species, and a global fit with standard deviation close to measurement accuracy was achieved with the program *XIAM*. Comparison to other toluene derivatives where a methyl group is in close proximity to a fluorine atom have shown that the barrier height of the three-fold potential is largely invariant at around 220 cm^{-1}.

Experimental Section

The microwave spectrum of 26DMFB was recorded in the frequency range from 2 to 40 GHz using two pulsed jet Fourier transform spectrometers with a coaxially oriented beam-resonator arrangement.[48,49] Some drops of 26DMFB were put on a piece of a pipe cleaner placed in front of the nozzle, and helium as carrier gas was passed over the sample at a stagnation pressure of 2 bar. The adiabatic expansion simultaneously reduces the collisional as well as Doppler line broadening. The strong rovibrational cooling of the molecules results in the population of only the lowest-lying rovibrational levels, which tremendously simplifies the observed spectrum.

Acknowledgements

The authors thank Prof. Dr. Wolfgang Stahl for providing the spectrometer for the measurements in the frequency range from 2.0 to 26.5 GHz and Prof. Dr. Martin Schwell for his help and support in the master thesis of S.K. at LISA. This work was supported by the Agence Nationale de la Recherche ANR (project ID ANR-18-CE29-0011).

Keywords: microwave spectroscopy • rotational spectroscopy • large amplitude motion • quantum chemical calculation • toluene derivative

[1] H. D. Rudolph, H. Dreizler, A. Jaeschke, P. Wendling, Z. *Naturforsch*. **1967**, *22a*, 940–944.
[2] W. A. Kreiner, H. D. Rudolph, B. T. Tan, *J. Mol*. *Spectrosc*. **1973**, *48*, 86–99.
[3] V. Amir-Ebrahimi, A. Choplin, J. Demaison, G. Roussy, *J. Mol. Spectrosc*. **1981**, *89*, 42–52.
[4] Z. Kisiel, E. Białkowska-Jaworska, L. Pszczółkowski, H. Mäder, *J. Mol Spectrosc*. **2004**, *227*, 109–113.
[5] V. V. Ilyushin, Z. Kisiel, L. Pszczółkowski, H. Mäder, J. T. Hougen, *J. Mol. Spectrosc*. **2010**, *259*, 26–38.
[6] S. Jacobsen, U. Andresen, H. Mäder, *Struct. Chem*. **2003**, *14*, 217–225.
[8] J. Rottstegge, H. Hartwig, H. Dreizler, *J. Mol*. *Struct*. **1999**, *478*, 37–47.
[7] H. D. Rudolph, A. Trinkaus, Z. *Naturforsch*. **1968**, *23a*, 68–76.
[9] K. P. Rajappan Nair, S. Herbers, J.-U. Grabow, A. Lesarri, *J. Mol. Spectrosc*. **2018**, *349*, 37–42.
[10] K. P. Rajappan Nair, S. Herbers, D. A. Obenchain, J.-U. Grabow, A. Lesarri, *J. Mol*. *Spectrosc*. **2018**, *344*, 21–26.
[11] K. P. Rajappan Nair, D. Wachsmuth, J.-U. Grabow, A. Lesarri, *J. Mol. Spectrosc*. **2017**, *337*, 46–50.
[12] K. P. Rajappan Nair, S. Herbers, J.-U. Grabow, *J. Mol*. *Spectrosc*. **2019**, *355*, 19–25.
[13] K. P. Rajappan Nair, M. K. Jahn, A. Lesarri, V. V. Ilyushin, J.-U. Grabow, *Phys*. *Chem*. *Chem*. *Phys*. **2015**, *17*, 26463–26470.
[14] K. P. Rajappan Nair, S. Herbers, D. A. Obenchain, J.-U. Grabow, *Can. J. Phys.* **2019**. DOI: 10.1139/cjp-2019-0477.
[15] M. Tudorie, I. Kleiner, M. Jahn, J.-U. Grabow, M. Goubet, O. Pirali, *J. Phys*. *Chem*. **2013**, A *117*, 13636–13647.
[16] L. Ferres, W. Stahl, H. V. L. Nguyen, *J. Chem*. *Phys*. **2018**, *148*, 124304.
[17] L. Ferres, K.-N. Truong, W. Stahl, H. V. L. Nguyen, *ChemPhysChe*m **2018,** *19*, 1781–1788.
[18] L. Ferres, J. Cheung, W. Stahl, H. V. L. Nguyen, *J. Phys*. *Chem*. **2019**, A *123*, 3497–3503.
[19] P. Groner, S. Albert, E. Herbst, F. C. De Lucia, F. J. Lovas, B. J. Drouin, J. C. Pearson, *Astrophys*. *J*. **2002**, *142*, 145–151.
[20] W. Neustock, A. Guarnieri, J. Demaison, G. Wlodarczak, Z. *Naturforsch*. **1990**, *45a*, 702–706.
[21] H. V. L. Nguyen and W. Stahl, *ChemPhysChem*, **2011**, *12*, 1900–1905.
[22] V. Van, J. Bruckhuisen, W. Stahl, V. Ilyushin, H. V. L. Nguyen, *J. Mol. Spectrosc*. **2018**, *343*, 121–125.
[23] V. Van, W. Stahl, and H.V.L. Nguyen, *Phys*. *Chem*. *Chem*. *Phys*. **2015**, *17*, 32111–32114.
[24] A. Jabri, V. Van, H. V. L. Nguyen, H. Mouhib, F. Kwabia-Tchana, L. Manceron, W. Stahl, I. Kleiner, Astron. *Astrophys*. **2016**, 589, A127.
[25] M. J. Frisch, G. W. Trucks, H. B. Schlegel, G. E. Scuseria, M. A. Robb, J. R. Cheeseman, G. Scalmani, V. Barone, G. A. Petersson, H. Nakatsuji, X. Li, M. Caricato, A. V. Marenich, J. Bloino, B. G. Janesko, R. Gomperts, B. Mennucci, H. P. Hratchian, J. V. Ortiz, A. F. Izmaylov, J. L. Sonnenberg, D. Williams-Young, F. Ding, F. Lipparini, F. Egidi, J. Goings, B. Peng, A. Petrone, T. Henderson, D. Ranasinghe, V. G. Zakrzewski, J. Gao, N. Rega, G. Zheng, W. Liang, M. Hada, M. Ehara, K. Toyota, R. Fukuda, J. Hasegawa, M. Ishida, T. Nakajima, Y. Honda, O. Kitao, H. Nakai, T. Vreven, K. Throssell, J.A. Montgomery, Jr., J. E. Peralta, F. Ogliaro, M. J. Bearpark, J. J. Heyd, E. N. Brothers, K. N. Kudin, V. N. Staroverov, T. A. Keith, R. Kobayashi, J. Normand, K. Raghavachari, A. P. Rendell, J. C. Burant, S. S. Iyengar, J. Tomasi, M. Cossi, J. M. Millam, M. Klene, C.

Adamo, R. Cammi, J. W. Ochterski, R. L. Martin, K. Morokuma, O. Farkas, J. B. Foresman, and D. J. Fox, Gaussian 16, Revision B.01, Inc., Wallingford CT, 2016.
[26] L. Ferres, W. Stahl, H. V. L. Nguyen, *Mol*. *Phys*. **2016**, *114*, 2788–2793.
[27] L. Ferres, H. Mouhib, W. Stahl, H. V. L. Nguyen, *ChemPhysChem*, **2017**, *18*, 1855–1859.
[28] H. V. L. Nguyen, *J. Mol*. *Struct*. **2020**, *1208*, 127909.
[29] H.V.L. Nguyen, J.-U. Grabow, *ChemPhysChem*. **2020**, *21*, DOI: 10.1002/cphc.202000234
[30] Z. Kisiel, O. Desyatnyk, L. Pszczółkowski, S. B. Charnley, P. Ehrenfreund, *J. Mol*. *Spectrosc*. **2003**, *217*, 115–122.
[31] W. Kohn, L. J. Sham, *Phys*. *Rev*. **1965**, *A 140*, 1133–1138.
[32] A. D. Becke, *J. Chem*. *Phys*. **1993**, *98*, 5648.
[33] C. T. Lee, W. T. Yang, R. G. Paar, *Phys*. *Rev*. **1988**, B 37, 785–789.
[34] L. Ferres, W. Stahl, I. Kleiner, H. V. L. Nguyen, *J. Mol*. *Spectrosc*. **2018**, *343*, 44–49.
[35] S. Grimme, J. Antony, S. Ehrlich, H. Krieg, *J. Chem*. *Phys*. **2010**, *132*, 154104.
[36] S. Grimme, S. Ehrlich, L. Goerig, J. Comp. *Chem*. **2011**, *32*, 1456–1465.
[37] J. C. López, V. Cortijo, S. Blanco, J. L. Alonso, *Phys*. *Chem. Chem. Phys*. **2007**, *9*, 4521–4527.
[38] C. Calabrese, A. Maris, L. Evangelisti, W. Caminati, S. Melandri, *ChemPhysChem*, **2013**, *14*, 1943–1950.
[39] V. Van, W. Stahl, M. Schwell, H.V.L. Nguyen, *J. Mol*. *Struct*. **2018**, *1156*, 348–352.
[40] Y. Zhao, D. G. Truhlar, Theor. *Chem*. *Acc*. **2008**, *120*, 215−241.
[41] R. J. Bartlett, M. Musial, *Rev*. *Mod*. *Phys*. **2007**, *79*, 291–352.
[42] P. R. Bunker and P. Jensen, Molecular Symmetry and Spectroscopy, 2nd ed.; NRC Research Press: Ottawa, Ontario, Canada (2006).
[43] H. Hartwig, H. Dreizler, Z. *Naturforsch*. **1996**, *51a*, 923–932.
[44] S. Herbers, S. M. Fritz, P. Mishra, H. V. L. Nguyen, T. S. Zwier, *J. Chem*. *Phys*. **2020**, *152*, 074301.
[45] M. Andresen, I. Kleiner, M. Schwell, W. Stahl, H. V. L. Nguyen, *J. Phys. Chem. A* **2018**, *122*, 7071–7078.
[46] M. Andresen, I. Kleiner, M. Schwell, W. Stahl, H. V. L. Nguyen, *ChemPhysChem* **2019**, *20*, 2063–2073.
[47] M. Andresen, I. Kleiner, M. Schwell, W. Stahl, H. V. L. Nguyen, *J. Phys. Chem. A* **2020**, 124, 1353–1361.
[48] J.-U. Grabow, W. Stahl, H. Dreizler, *Rev*. *Sci*. *Instrum*. **1996**, *67*, 4072–4084.
[49] I. Merke, W. Stahl, H. Dreizler, Z. *Naturforsch*. **1994**, *49a*, 490–496.

Entry for the Table of Contents

FULL PAPER

Combined experimental and computational study of the torsion-rotation spectrum produced by the internal rotations of two equivalent methyl groups yielded highly accurate torsional barrier and geometry parameters of the C_{2v} molecule 2,6-dimethylfluorobenzene, serving as a model system for testing and further development of program codes and group theory.

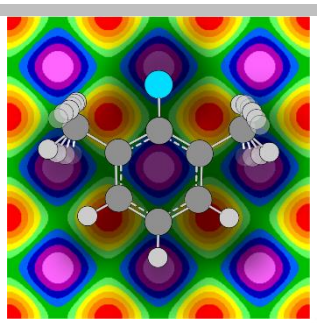

*S. Khemissi, Dr. H. V. L. Nguyen**

Page No. – Page No.

Two Equivalent Internal Rotations in the Microwave Spectrum of 2,6-Dimethylfluorobenzene